Measurement 243 (2025) 116439

Contents lists available at ScienceDirect

Measurement

journal homepage: www.elsevier.com/locate/measurement

Encapsulated UHF antenna for early and long-term concrete monitoring

N. Vidal [a,*], J.M. Lopez-Villegas [a], I. Cairó [b], A. Garcia-Miquel [c], J. Romeu [d], L.L. Jofre [d]

[a] Department of Electronic and Biomedical Engineering, RF Group, University of Barcelona/UB, 08028 Barcelona, Spain
[b] WitekLab, 08223 Terrassa, Spain
[c] Institut de Neurociencia avançada Barcelona/ INAB, 08039 Barcelona, Spain
[d] CommSensLab, Technical University of Catalonia/UPC, 08028 Barcelona, Spain

ARTICLE INFO

Keywords:
Concrete Monitoring
Structural Health Monitoring
UHF antenna
Sensor
Additive manufacturing
RFID

ABSTRACT

This paper introduces a novel encapsulated 3D-printed UHF antenna system for early-stage and long-term concrete monitoring. Our goal is to leverage the capacities of additive manufacturing techniques to enhance antenna performance. We design and implement an encapsulated biconical geometry to mitigate medium losses due to being placed within concrete, to improve radiative efficiency, and to ensure stable antenna impedance. Various antenna prototypes were designed, optimized, fabricated, and characterized via laboratory and mortar sample measurements. We succeeded in integrating our novel system with existing temperature and humidity sensors, and interfaced it with an automatic data acquisition system for continuous concrete monitoring. Comparison with previous acquisition systems was performed. Herein, we present the design process, laboratory characterization, and field testing, including three case studies. Significant efforts were made to miniaturize the antenna while maintaining performance. Full system integration is demonstrated. Measurements were taken from antennas buried at depths of up to 30 cm; they showed good performance from an early start and up to long-term operation. These promising results confirm that improved antenna design and proper encapsulation can enhance system performance, especially in challenging and dynamic environments such as concrete.

1. Introduction

The versatility, affordability, and strength of concrete make it the most widely used construction material in the world. In 2023 global production was estimated at 3.8 billion metric tons [1]. However, its true potential is only unlocked after proper curing, which is heavily dependent on temperature and humidity [2]. By closely monitoring these factors during hydration (the chemical process by which concrete hardens), engineers can ensure the smooth running of this aspect of their projects. This translates to a safe, durable final structure and allows for better planning of construction timelines by predicting curing and drying rates. While temperature and humidity are crucial, other parameters like corrosion rate, pH, and strain/stress/crack development are also important for long-term performance [3].

Concrete testing techniques can be divided into two main categories: destructive and non-destructive. Each offers advantages and drawbacks depending on the information required and the stage of the lifecycle of the concrete involved [4]. A specific testing method is chosen based on the needs of the project and the information to be collected. In recent years, interest in non-destructive techniques has increased, particularly for monitoring concrete in its early stages. Techniques using microwaves, which can penetrate concrete, have been devised to analyze the hydration process [5], characterize dielectric and reflection properties [6,7], and monitor the compressive strength [8], among other applications [4].

Radio frequency identification (RFID) systems use radio waves for wireless communication between tags attached to objects and readers that capture data. The reader emits radio waves that activate the tag, which then transmits its stored information (like a unique ID or sensor readings) back to the reader. These data are then sent to a computer system for further processing. In this way, identification and tracking can be performed automatically without the need for line-of-sight scanning. In the context of concrete monitoring, RFID technology offers a particularly promising tool since RFID tags can be designed to withstand harsh conditions, such as extreme temperatures, corrosive chemicals, and moisture. Therefore, while traditional RFID technologies might not be directly applicable to monitoring concrete hydration, specially designed tags can be embedded in the concrete and data can be tracked wirelessly [9]. This potentially enables not only tracking and data collection, but also fully autonomous external monitoring.

* Corresponding author.
E-mail address: nvidal@ub.edu (N. Vidal).

https://doi.org/10.1016/j.measurement.2024.116439
Received 7 October 2024; Received in revised form 3 December 2024; Accepted 5 December 2024
Available online 6 December 2024

Embedding sensors in concrete for structural health monitoring presents numerous challenges [10]. Several highly promising proposals have been presented recently showing good results for concrete monitoring, specifically using the UHF band. Some work focuses on monitoring structural integrity [11–14], while other research focuses on more specific measurement of temperature, humidity or other characteristics [15–18]. Some of the proposals focus only on early-stage monitoring [19] and in this context, obtaining reliable readings from the start of the hydration process presents major challenges due to significant changes in attenuation losses and the electrical properties of the concrete. Monitoring humidity and temperature within concrete during the early stages, particularly during curing, is vital for several reasons directly related to the final strength and integrity of the structure. Accurate monitoring allows the hydration process to be controlled, cracking to be minimized, and strength development to be optimized, as well as facilitating quality control and predicting future performance. Finally, recent advances in embedded technologies and self-sensing concrete for structural health monitoring have been presented [20], together with a state-of-the-art review of monitoring enabled by RFID technology [21].

Within such a context, providing both early and long-term monitoring is a major challenge. The relative permittivity of concrete may range from 20 to 4 in the UHF band [16,22,23], which means that the design of the antenna attached to the sensor is a key factor. An ideal antenna, when embedded, should function well regardless of these variations in permittivity (dielectric constant) and conductivity. This requires a good match (efficient power transfer) to be maintained across a range of values and also the potential to adapt to temporal changes. Some of the works cited point out the limitations regarding measurements taken during the first hours after laying the concrete [15–17]. Encapsulating the antenna is a potential solution, as explored in previous research for applications other than concrete [24,25]. A recent paper [26] discusses the challenges of antenna design for concrete-embedded systems. Those authors propose a patch antenna design, analyze different shielding materials, and highlight the challenge posed by miniaturization while maintaining performance.

In light of the foregoing discussion, the aim of this study is to enhance concrete measurement capabilities through the introduction of a novel antenna design. The antennas employed in previous related work have been planar in nature. In contrast, we propose a fully three-dimensional conical antenna fabricated using additive manufacturing (AM) processes. The production of antennas using modern AM techniques has attracted the attention of different research groups [27]. The initial antenna design presented in this paper originated from preliminary general analysis of the state of the art [28]. By leveraging full 3D-printing techniques, in the present work we have been able to overcome the limitations of planar designs and fabricate models that exhibit increased compactness while enabling complete system integration. We present the design process and characterization of an encapsulated miniaturized UHF antenna capable of providing both early and long-term measurements to optimize structural health monitoring. The antenna is entirely 3D printed and is designed to operate embedded within concrete while fully integrated with a sensing module. This embedded system allows continuous monitoring of temperature and humidity inside concrete right from the start of the hydration process. Furthermore, a specifically designed packaging solution incorporating a dielectric coating is proposed to minimize impedance changes when the antenna is embedded within concrete. It has been shown that confining the reactive near-field within the packaging mitigates medium losses and thereby maximizes radiation efficiency [29]. We specifically address the whole design of the antenna and its characterization inside concrete.

After an optimization process, the antenna is seamlessly integrated with temperature and relative humidity sensors. This integrated system is interfaced with an automatic data acquisition system designed for continuous concrete monitoring. The system into which the new antenna design was integrated is "MONSEC", a new temperature and

a

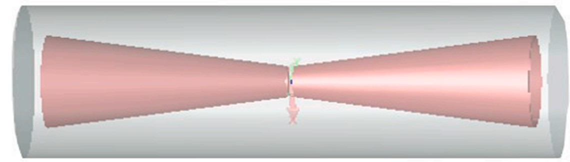

b	Geometry
cone angle	30 degrees
encapsulation radius	12 mm
encapsulation length	60 mm
	Materials
metal conductivity (bulk copper)	5.8 10^7 S/m
dielectric permittivity	2.9
dielectric loss tangent	0.02
mimicking concrete liquid permittivity	4-18
mimicking concrete liquid loss tangent	0.3-0.6

c

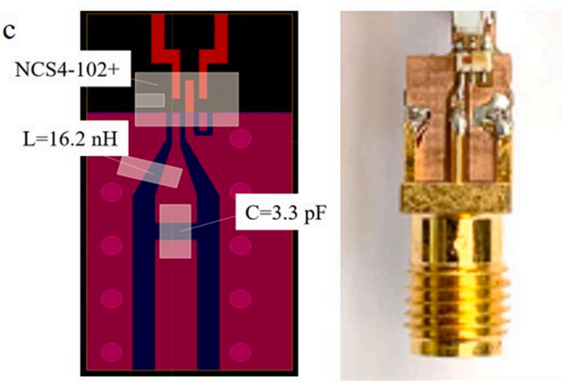

Fig. 1. CAD model of the biconical antenna (a); and main design parameters (b), together with single-ended to differential balun connector (c).

humidity sensor developed by "WitekLab" and "Smart Engineering" [30,31]. The integrated system allows live monitoring of these magnitudes by embedding a network of sensors inside the maturing concrete. Compared to previous acquisition systems, the new design incorporating the novel antenna and sensors is capable of measuring temperature and humidity as soon as it is deployed, for both extremely early and long-term operation. The entire system has been tested in both laboratory and field environments to assess its performance.

The rest of this paper is organized as follows. In Section 2 we present the methodology, antenna design, characterization, and manufacturing process, including an initial test of the prototype in mortar. Section 3 contains a discussion of the miniaturization process using 3D printing techniques, including full integration of the system and measurements. Finally, Section 4 presents our main conclusions.

2. Methodology and preliminary Investigations

This section details the design and characterization process of the preliminary encapsulated UHF antenna for taking concrete measurements. It is crucial to emphasize that the methodology employed throughout this and the following sections, considers the subsequent integration of the antenna with the electronics board and sensors of the "MONSEC" system.

2.1. Methods

First, we designed a biconical antenna prototype to assess the optimal radiation scenario, confirm the feasibility and impact of

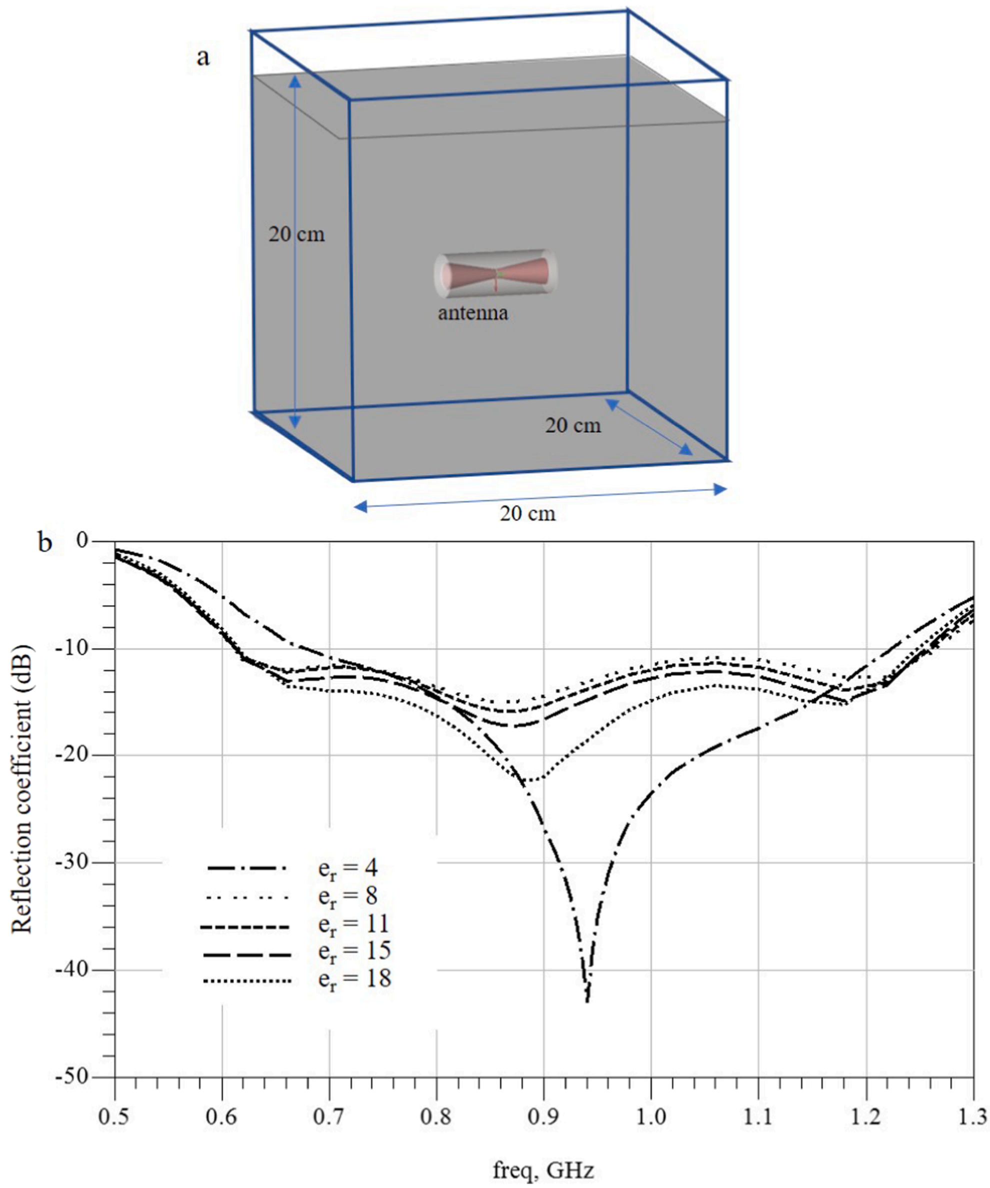

Fig. 2. a) the modeling and measurement set-up. b) simulated reflection coefficient as a function of frequency with the antenna immersed in different liquids emulating the electrical properties of concrete at various stages of curing.

encapsulation, and establish a baseline for subsequent miniaturization efforts. Unlike traditional planar designs (e.g., dipolar, loop, and patch antennas) commonly used in UHF applications [11–15], a biconical geometry was selected for its potential to retain the reactive near-field within the packaging after encapsulation. This could mitigate medium losses that affect radiative efficiency and ensure stable antenna impedance when submerged in concrete. Cylindrical encapsulation was added around the antenna. Based on prior theoretical analysis, we determined the radio length, demonstrating the optimum radius for impedance stability [25]. The final geometry and primary design parameters are illustrated in Fig. 1a, b.

It is important to note that the electronic board in the "MONSEC" system was designed to attach to a single-ended-fed antenna with a reference impedance of 50 Ω. However, the biconical antenna design is intended for differential excitation; and the impedance of the biconical antenna is not 50 Ω. Therefore, to integrate the biconical antenna design into the "MONSEC" system, some additional components were required. The first of these was a balun to make the conversion from differential excitation to single-ended excitation. We chose a monolithic balun, the Low Temperature Cofired Ceramic (LTCC) Transformer NCS4-102 + from Mini-Circuits, because of its reduced size and optimized performance in the 700 MHz to 1 GHz frequency range, which includes our target UHF frequency of 867 MHz. Note that while the balun is very effective at converting differential excitation to single-ended excitation, it does not adapt the single-ended impedance to the specified value of 50 Ω. Accordingly, in addition to the balun, reactive components such as capacitors and inductors were also required to ensure impedance matching. For this, we used a parallel capacitor and series inductor matching network, constructed with 0603 SMD devices. Fig. 1c is a picture of the whole balun and matching network.

Full wave electromagnetic simulations were performed to model the entire antenna, balun, and encapsulation assembly within a simulated concrete environment. Various liquids emulating the electrical properties of concrete were considered. The simulation setup is illustrated in Fig. 2a. The simulations examined relative permittivity values ranging from 4 to 18, using electrical parameters derived from concrete permittivity and conductivity data analyzed in a previous study [32]. The results, based on reflection coefficient analysis and overall radiation

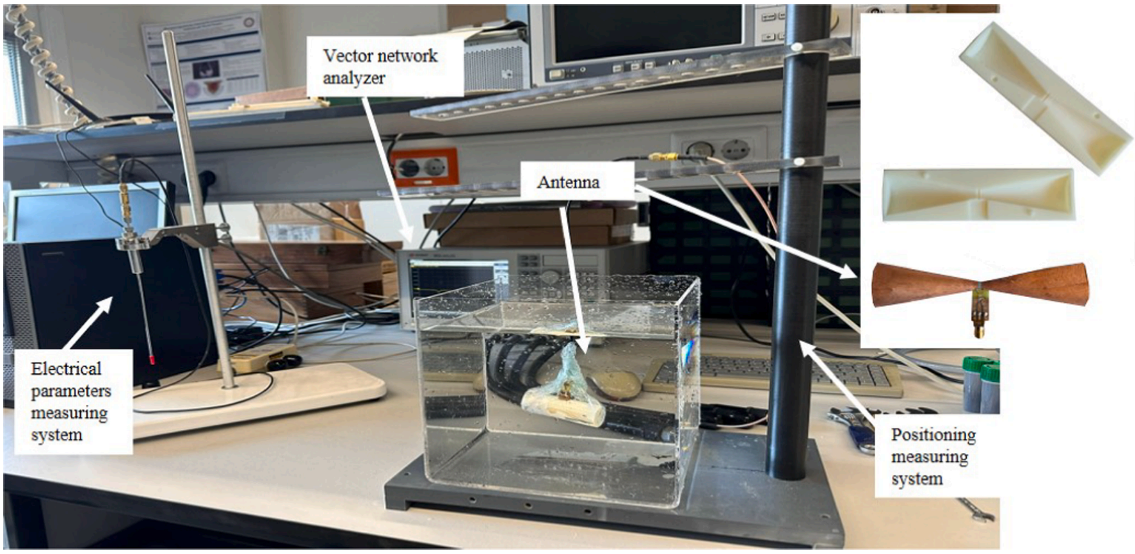

Fig. 3. Laboratory setup for measurements of the reflection coefficient of the antenna prototype and encapsulation inside the liquid mimicking concrete.

performance, are presented in Fig. 2b. The simulated reflection coefficient data for different electrical parameters of concrete exhibited good stability, leading to the selection of the cylindrical encapsulation geometry for subsequent designs.

Once the 3D model assembly was numerically validated, we began the manufacturing process with the fabrication of the antenna and encapsulation. The parts were printed using an Objet260 Connex 1 3D printer from Stratasys, Ltd. As the printing material, we used a photopolymer which, after UV curing, has a relative permittivity of 2.9 and a loss tangent of 0.02. A silver ink was used as a seed to grow a layer of copper by electroplating in the biconical parts. The same procedure has previously been used by our research group to implement conical inductors, 3D capacitors, broadband impedance transformers, and filters, among other components. A detailed description of the fabrication process can be found in [33]. The final prototype is shown in Fig. 3 together with the laboratory measurement setup.

To match the simulated conditions and take measurements in the laboratory, a cubic container was filled with various homogeneous solutions. Four solutions were formulated to mimic the time-dependent changes in the electrical properties of concrete. The solution permittivity and conductivity values were derived from previous analysis of the concrete setting process [16]. The recipes themselves were based on prior research on the dielectric properties of aqueous and organic liquids [34], where the authors performed experimental analysis of effective permittivity for a range of ethanol solutions. Inspired by that work, we produced and tested different ethanol and xylene-based solutions to see how they mimicked the electrical parameters of concrete. Characterization of the solutions was performed using an Agilent Technologies 85071E commercial complex permittivity measurement system, along with an HP8720C vector network analyzer and the accompanying software. The system utilizes a coaxial open-ended probe inserted into the cuboid shell filled with the liquid solution. Calibration involves measuring open, short, and water standards at 20 °C. The entire setup is presented in Fig. 3. The experimental results of the antenna design for a specific concrete stage ($\varepsilon_r = 18$) are displayed alongside the corresponding simulated data in Fig. 4. There is good agreement between the measurements and the simulated data in this case; a similar degree of agreement was found for the remaining concrete electrical values.

2.2. Integration with the “MONSEC” system

The “MONSEC” system incorporates a compact, silicon-based integrated circuit (EM4325-IC [35]) capable of sensing both temperature and relative humidity, a bow-tie broadband antenna, and a 3D-printed PLA casing. It is crucial to note that the sensor unit is integrated into the remaining electronic system, with particular attention paid to ensuring that the placement of the sensor IC minimizes discrepancies between the humidity and temperature conditions of the test environment and those surrounding the sensor. The influence of heat generated by nearby devices or the sensor itself must also be considered [17]. The sensor operates reliably in condensing environments, offering an operating range of [0, 100 % RH] and [-40, +125 °C]. Relative humidity and temperature accuracies are ± [1.5, 1.8 % RH] (30–70 % RH) and ± 0.1 °C, respectively. For RH > 70 %, the accuracy tolerance is ± [2, 3 % RH]. A commercially available RFID reader system, equipped with a circularly polarized patch antenna and a Nordic ID eNUR-10 W reader [36], was positioned externally to systematically collect data from the embedded sensors. In this study, as a preliminary test, the standard antenna was replaced with our newly developed encapsulated antenna. A coaxial cable with SMA connectors was used to establish the connection.

2.3. Mortar setup and measurements

Mortar cubes were procured from PROCOMSA, a concrete contractor specializing in construction concrete supply and pouring. The mortar mix was formulated to replicate the typical composition of mortar surrounding coarse aggregate in standard concrete. A dry-mixing procedure outlined in reference [37] was followed that involved thoroughly dry-mixing all the solid components (cement, sand, and gravel) before incorporating the water. After mixing, the fresh mortar was cast in 80 x 80 x 80 cm molds.

The recording stations were positioned in alignment with the mortar at various distances, as illustrated in Fig. 5a. The tests were conducted concurrently with the company’s own routine testing procedures. In other words, our prototypes were integrated alongside their standard sensors within the mortar. The encapsulated antenna was connected directly to the electronic board and sensors via a coaxial cable, as depicted in Fig. 5b.

An enlarged view of the interior of the mortar illustrates the spatial arrangement of the various devices (Fig. 5c). For this initial measurement, we incorporated two of our new modules. The commercially available “MONSEC” modules (indicated by red boxes in Fig. 5a) were positioned at depths of 7.5, 15, and 30 cm. Our two newly designed modules were placed at the deepest positions (30 cm) to assess the worst-case scenario. It is important to note that metal bars were also

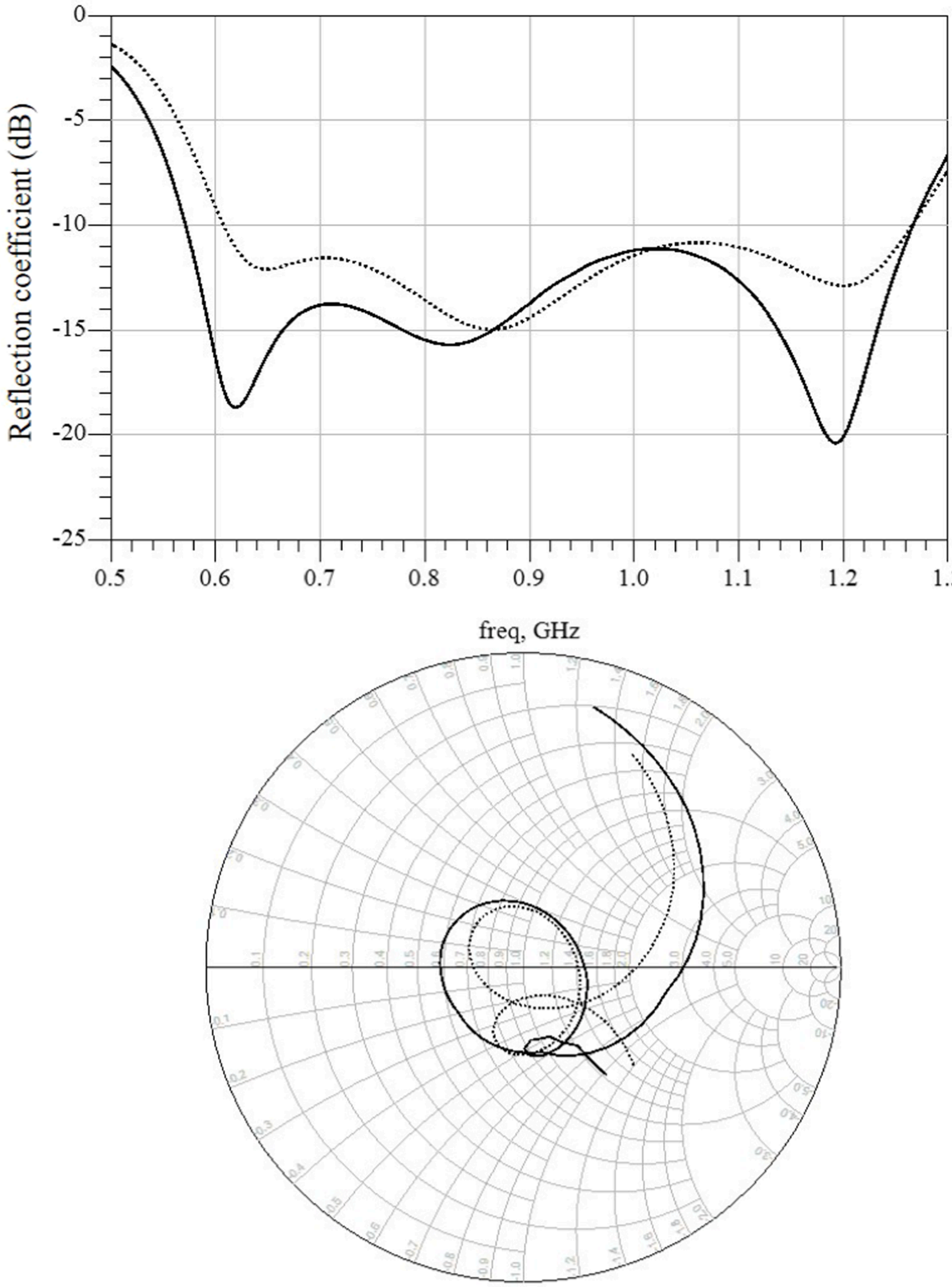

Fig. 4. Simulated (dotted line) and measured (continuous line) reflection coefficient of the antenna for a surrounding liquid with an electric permittivity of 18.

inserted into the cubes to stabilize the units, as is typical in actual construction uses, as such metal bars could potentially impact the performance of the antenna assemblies. To address this concern, we simulated different scenarios with one, two or three bars close to the antenna. Different locations and orientations were tested. The modeling results confirmed that the overall effect was minimal. Minor discrepancies were observed compared to the baseline case without the metal bars.

For precise analysis and to isolate the performance of the proposed new antenna assembly, only the biconical antenna and its encapsulation were placed inside the mortar during this preliminary test: the electronic board and sensing module were kept outside. Fig. 5c shows the initial configuration, with our prototypes covered by white plastic and only the antenna assembly embedded in the concrete. Finally, Fig. 5d shows the final setup with the electronic board and sensors positioned outside the cubes while the antenna is embedded in the mortar. To analyze the impact of residual radiation from the electronic unit on measurement accuracy, the new antenna was disconnected. No signal was recorded, confirming that the antenna is the primary source of the signal.

In the complete system, the wireless sensor measures and transmits temperature and relative humidity data for both fresh and hardened concrete. The data are sent via a radio signal to a central recording station which acts as an external reader, receiving sensor data, storing it locally, and then forwarding it to a cloud server. The station can be powered by the electricity grid or a battery with options for grid or solar charging. According to the connectivity at the project location, the data transmission method can be: a Wi-Fi network with internet access, a GPRS/3G/4G/LTE modem, or manual downloading of data to a USB device. Cloud-based information is accessible 24/7 and updates every 15 min. The reader unit utilizes the commercially available Nordic ID eNUR-10 W reader to connect wirelessly to a computer system and transmit processed data. The automatic data acquisition system supports high-precision and real-time data monitoring. The data acquired by the

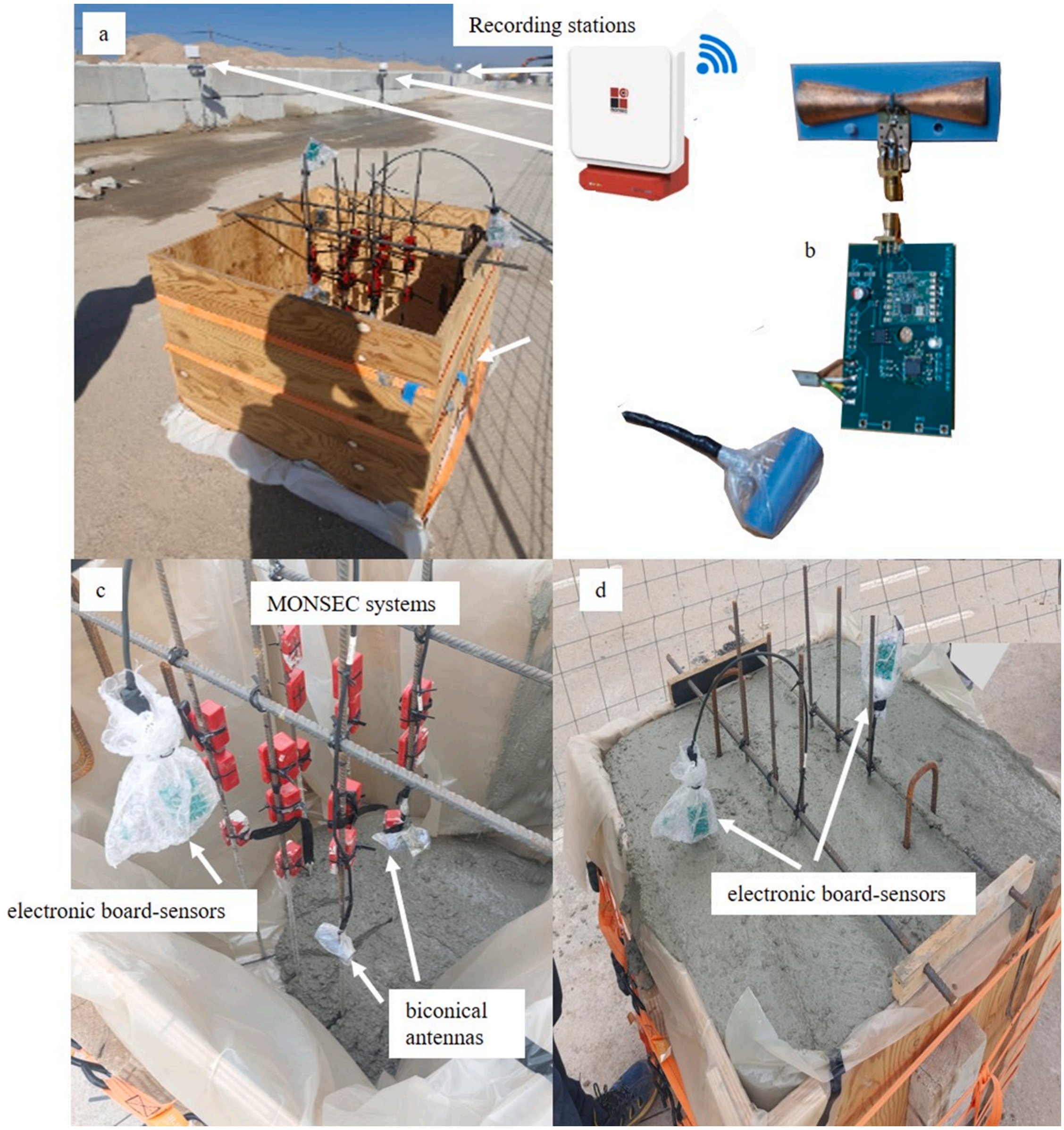

Fig. 5. A) preliminary view of a mortar cube and measurement setup. b) image of the electronic board and antenna connections. c) enlarged view of the "monsec" systems distribution (in red), together with two biconical antennas. d) final view of the mortar. (For interpretation of the references to colour in this figure legend, the reader is referred to the web version of this article.)

sensors are automatically sent to the cloud, via a receiving station connected to the data network. Once in the server, there are several algorithms that treat the data and when a user is logged into a platform, the processed data are shown in real time. Data are stored in a mySQL database and will always be available for the user at any time.

Fig. 6 presents temperature measurements for two devices over four days. The results of the company's standard system are compared to the performance of the new antenna system. While the regular system yielded no results during the first 14 h of operation, the proposed new module can take measurements from the beginning of the observation period. The curves diverge because, as previously explained, it was deemed appropriate to keep the sensor of the new system outside the cube. Consequently, this preliminary measurement taken using the new module does not reflect the behavior of the concrete but rather diurnal and nocturnal temperature fluctuations. As mentioned earlier, we considered it crucial to follow this methodology initially in order to characterize the antenna, assess its performance, compare it to simulations, and definitively isolate sources of error unrelated to the proposed module. In the next section we present the completely integrated antenna and sensor system operating within the mortar cube.

3. Full system integration

3.1. Miniaturization and measurements

Following the analysis reported in previous sections and prior to final integration of the encapsulated antenna into the system, it was essential to explore the feasibility of miniaturizing the device while maintaining performance. Our target size matched the dimensions of the "MONSEC" electronic board and case.

While preserving the biconical geometry, we integrated two symmetrical spiral radiators, as illustrated in Fig. 7a. These radiators enabled the effective length of the antenna to be maintained while reducing the overall size of the device. The encapsulation radius remained identical to the first prototype for stability purposes. Applying the methodology outlined in Section 2, the new antenna was optimized,

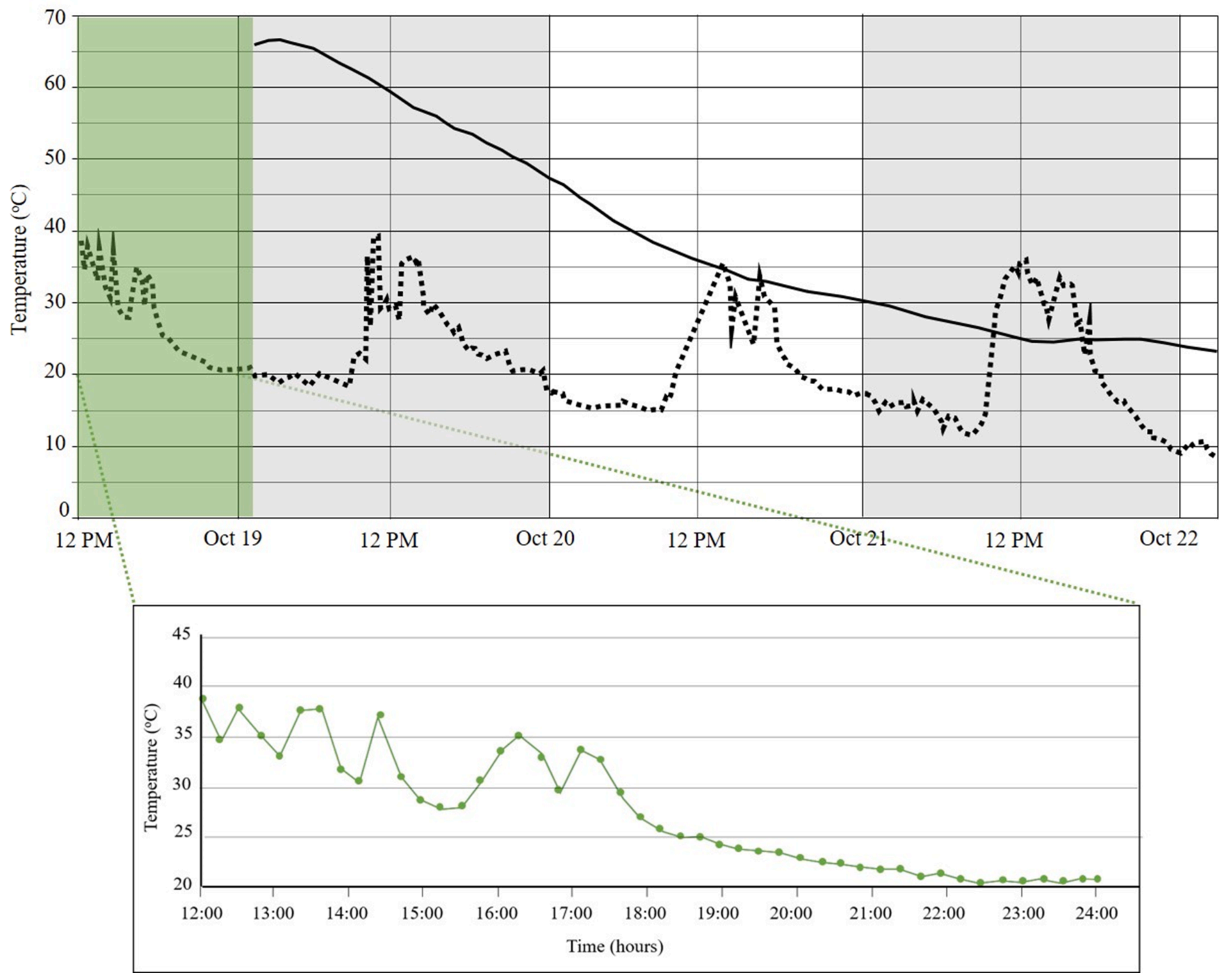

Fig. 6. Temperature measurements over the first 4 days after deployment for the regular "MONSEC" system (continuous line) and the new system with the biconical antenna (dashed line). The green area indicates the measurement gap for the regular system covered by the new system. (For interpretation of the references to colour in this figure legend, the reader is referred to the web version of this article.)

a balun was added, and laboratory measurements were taken. Fig. 7 presents the manufactured antenna module with its key geometric parameters. The modeled and measured reflection coefficients of the prototype over the target frequency band are shown in Fig. 7c for a relative permittivity of 18. Excellent agreement between simulations and measurements was observed. Furthermore, the new spiral antenna proved to be stable when immersed in liquids of varying dielectric constant. As expected, miniaturization resulted in a significant bandwidth reduction. However, the measured bandwidth across different tests ranged from 140 to 190 MHz. This large bandwidth ensures stability in the face of variations in the relative dielectric constant that occur at different stages of the concrete curing process, thus maintaining long-term stability.

To assess the overall performance of the new prototype, we also took measurements in mortar, again mirroring the methodology in Section 2. As for the initial measurements, the sensor was positioned outside the concrete while the antenna was embedded alongside the company's commercial sensors. The experimental data are presented in Fig. 8. Again, excellent performance was confirmed, with measurements available from the outset. Fig. 8 also highlights differences compared to the regular commercial module. Variations in temperature ranges relative to the preliminary approach (Section 2.2) are attributed to seasonal differences: the first experiments were conducted in October 2023, the second in January 2024.

3.2. *Final integration and measurements*

Considering all the previous results, we next set about fully integrating the new antenna into the "MONSEC" system. Our first proposal minimized changes to the company's standard system. So, we worked under significant constraints in terms of size and maintaining the electronic board and sensors distribution the same. Fig. 9 presents a schematic of this initial integration, accompanied by images of the modules we prepared. The electronic board remained unchanged, while the antenna and balun were directly soldered with a 90-degree bend. To ensure waterproofing and corrosion resistance of the encapsulated antennas, especially when employed for long-term applications, the enclosures were IP67 compliant. In addition, we applied grease specifically to protect the metal connectors from corrosion and used rubber washers to make sure all the external connectors were well sealed.

In this case, no laboratory tests were conducted; instead, the prototype was directly tested in the field. Fig. 10 shows an image of the new devices in yellow boxes at different depths inside the mortar cube. Measurements were collected following the same methodology introduced in previous sections. The temperature results over the first 24 h of operation are presented for one of the prototypes. The tests were conducted in July 2024. As can be observed, again we obtained measurements from the very beginning of operation, so we now confirmed the performance of the encapsulated antenna with the whole system inside the concrete.

This was our first attempt at producing a commercial product and we a

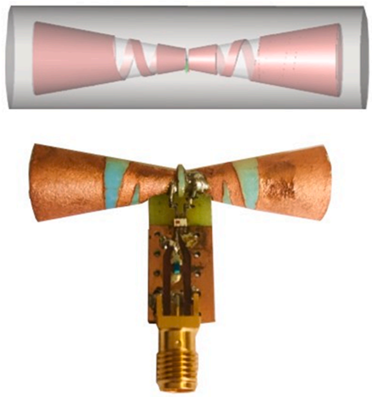

b

Geometry	
cone angle	30 degrees
encapsulation radius	12 mm
encapsulation lenght	50 mm
metal strip width	2 mm
pitch between turns	4 mm
Materials	
metal conductivity (bulk copper)	5.8 10^7 S/m
dielectric permittivity	2.9
dielectric loss tangent	0.02
mimicking concrete liquid permittivity	4-18
mimicking concrete liquid loss tangent	0.3-0.6

c

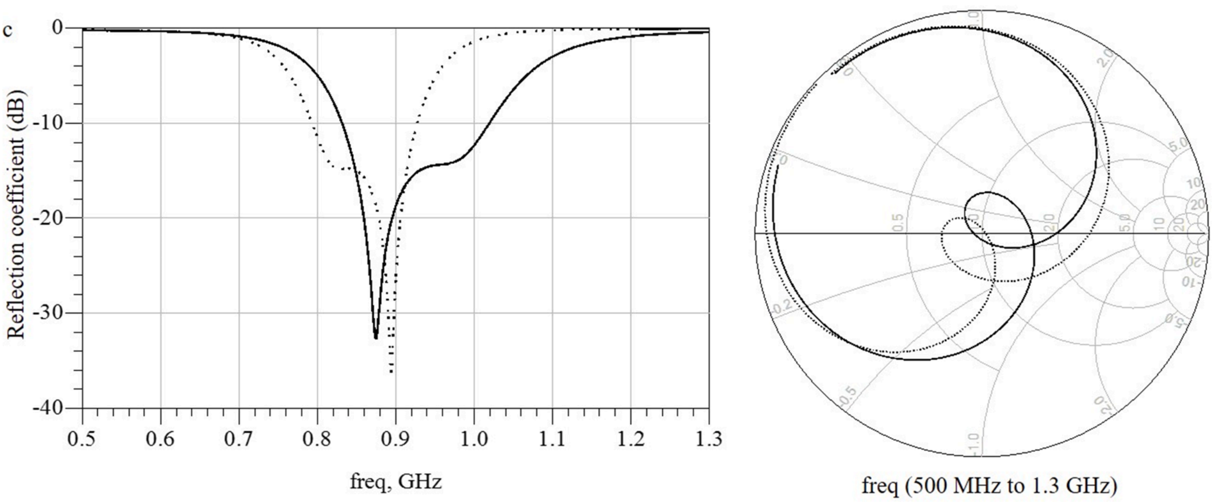

Fig. 7. CAD model and manufactured spiral antenna (a); and main design parameters (b), together with simulated (dotted line) and measured (continuous line) reflection coefficient of the antenna for a surrounding liquid with an electric permittivity of 18. (c).

believe the results were promising. Nevertheless, 2 of the 4 antennas we deployed did not work properly and we decided to address some issues. We believe that the distribution used was the simplest and quickest option for initial industrial implementation, but clearly it was not optimal and left significant room for improvement. We concluded that trying to capitalize on the existing distribution was not the best approach and that various changes could be introduced to enhance performance. Specifically, the box design should be modified to allow the antenna to be connected in the same plane as the board; in the initial full prototype system used to take the previous measurements, it was positioned at a 90-degree angle. Eliminating this abrupt change in connection should be beneficial. Additionally, the battery should be relocated away from the antenna. In the previous test it was directly attached to the antenna, which could well interfere with its operation. Moreover, the box components should also be adjusted to accommodate the antenna encapsulation while minimizing the air gap. We also noticed that for insulation purposes, epoxy resins were used in the area where the board connects to the balun. It seems that these resins may have come into contact with the balun, potentially altering the matching network, which could explain the malfunctioning of some of the antennas we observed. Despite these challenges, the prototype functioned, and we believe there is considerable potential for improvement. The company providing the “MONSEC” solution has informed us that these tests have formed the basis for a next-step product improvement. Their aim is to achieve good communication with sensors at deep locations, as much as 40 to 50 cm deep, from the time the sensor is deployed.

4. Conclusions

In this work, we present a miniaturized encapsulated UHF antenna for non-destructive early-stage and long-term structural concrete monitoring. Novel 3D additive manufacturing techniques offer new possibilities for improving the performance of electronic devices, especially antennas operating in challenging environments such as within concrete. We designed, optimized, produced, and characterized various antenna prototypes, conducting measurements in the lab and on three mortar samples. We chose an encapsulated biconical geometry due to its potential to confine the reactive near-field within the encapsulation, a technique already proven to be effective in other applications though not yet in concrete. This approach was expected to mitigate medium losses, enhance radiative efficiency, and ensure stable antenna impedance. A cylindrical encapsulation was added around the antenna. Proper cylinder design paying special attention to the radius is essential to minimize antenna detuning. To achieve miniaturization while maintaining performance, we adopted a spiral geometry and tailored the encapsulation accordingly. Due to their versatility and capacity to produce complex 3D structures, 3D printing techniques were employed to fabricate the prototypes.

We modeled various scenarios during the design process and replicated them in the laboratory. To simulate the time-dependent electrical properties of concrete, we formulated liquid solutions with permittivity and conductivity values derived from previous research. We also made the necessary adjustments to integrate the antenna with the sensing unit, which required a balun to convert from differential excitation to single-ended excitation, together with the incorporation of reactive components such as capacitors and inductors to ensure impedance matching.

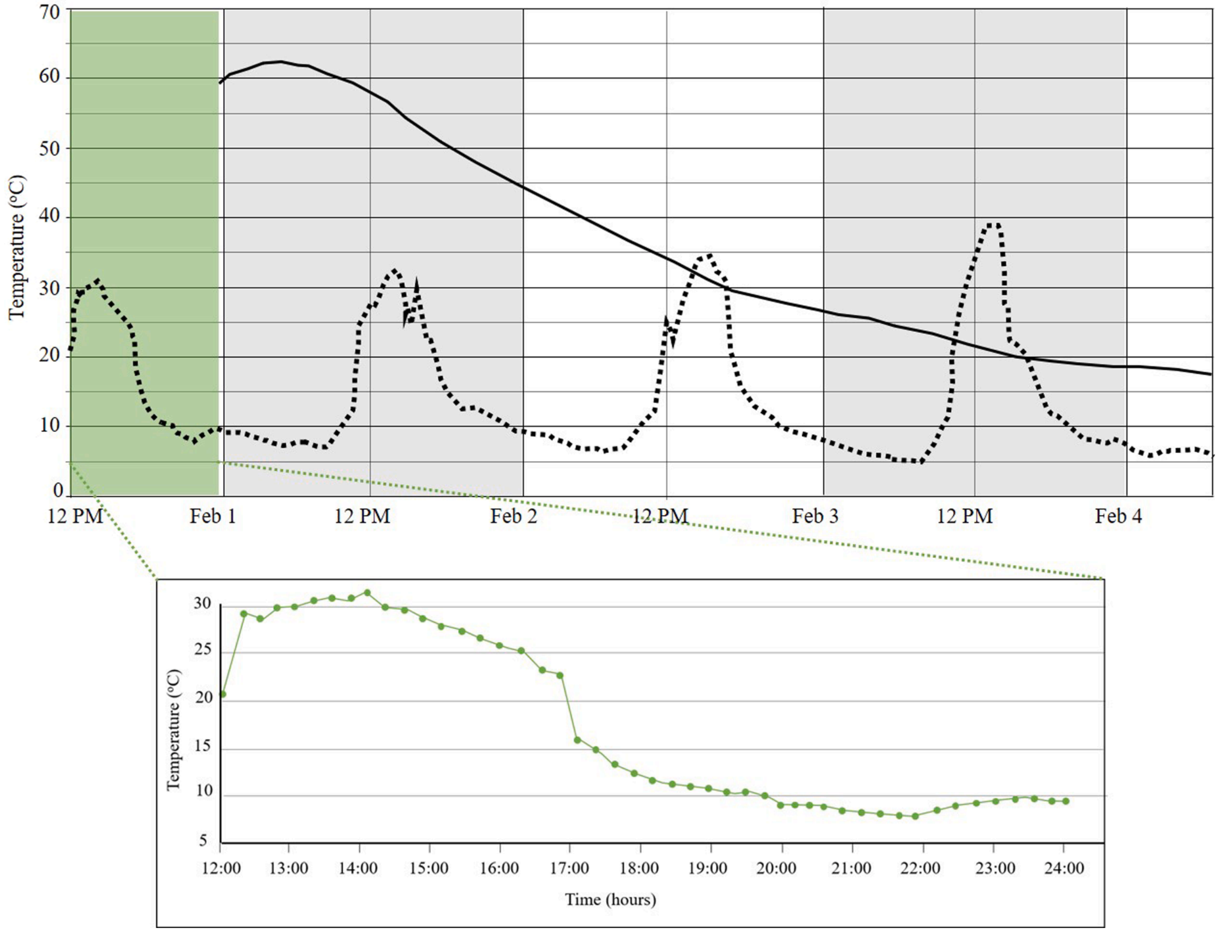

Fig. 8. Temperature measurements over the first 4 days after deployment for the regular “MONSEC” system (continuous line) and the new system with the biconical antenna (dashed line). The green area indicates the measurement gap for the regular system covered by the new system. (For interpretation of the references to colour in this figure legend, the reader is referred to the web version of this article.)

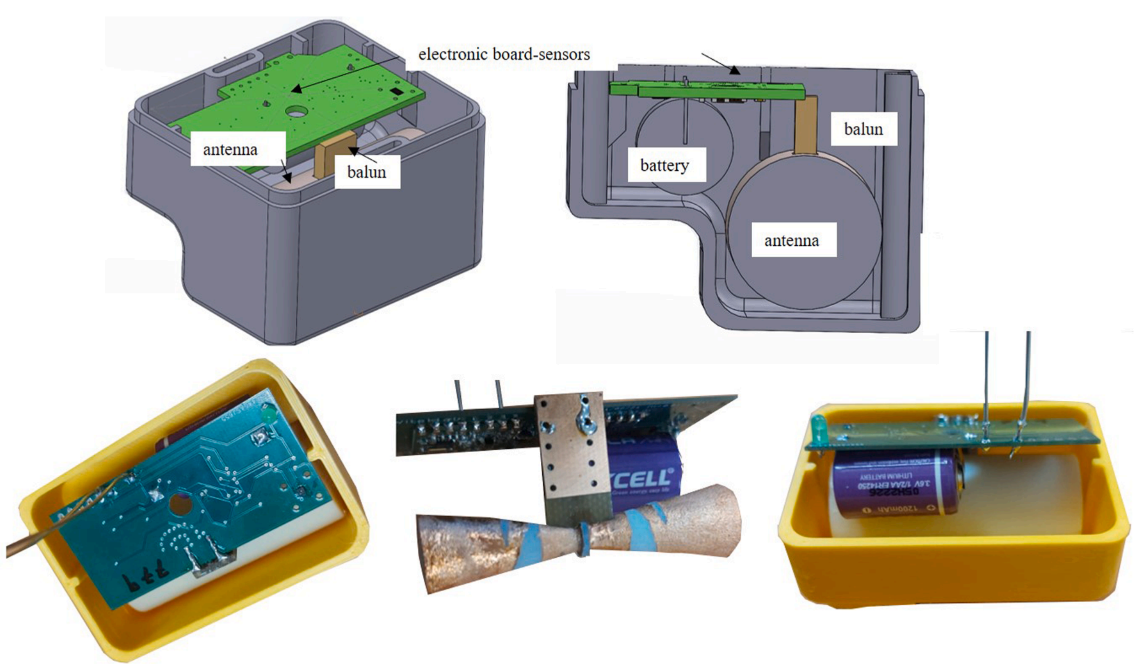

Fig. 9. Schematic and prototype images of the encapsulated spiral antenna integrated into the “MONSEC” system.

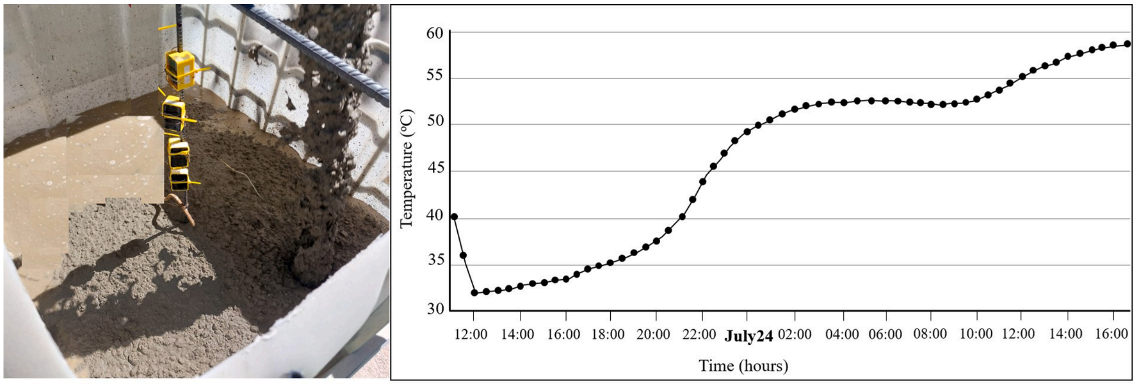

Fig. 10. View of a mortar cube and the measurement setup (left) and results of temperature measurements for the first 30 h of one of the systems (right).

Simulated and measured data agreed well, confirming the stability of the antenna under different conditions. At this point, we partially integrated the antenna and encapsulation system with the temperature and humidity sensors using a pre-existing module developed by the companies "Witeklab" and "Smart Engineering". While their module already incorporated an antenna, it had encountered issues, particularly within the first 24 h of operation. Our new antenna system improved measurements and provided data from the beginning of operation, thereby validating the feasibility and performance of our proposed geometry. Additionally, our prototypes were placed at considerable depths, up to 30 cm inside the concrete, and demonstrated improved communication ranges. Finally, automatic data acquisition was implemented to support high-precision, real-time monitoring.

Preliminary full system integration was proposed with the goal of minimizing modifications to the company's existing system, resulting in significant constraints on size and the need to maintain the electronics unaltered. This initial implementation functioned correctly. However, we identified several issues and determined that further development is needed for robust system integration. Based on this collaboration, we are glad to hear that our research has helped "Witeklab" improve sensor performance in line with the goals announced before. That development is currently under industrial protection.

Future work should focus on optimizing the system and addressing the issues identified in the initial integration. This includes improving the casing design and component layout. Additional testing at greater depths is also needed. Finally, slightly larger antennas could enhance the overall robustness of the system.

Our multidisciplinary approach, encompassing design, testing, and full system integration, yielded promising results that support the initial hypothesis. Proper antenna encapsulation can enhance system performance, especially in challenging and dynamic environments like concrete.

CRediT authorship contribution statement

N. Vidal: Writing – review & editing, Writing – original draft, Visualization, Validation, Supervision, Software, Project administration, Methodology, Investigation, Funding acquisition, Formal analysis, Conceptualization. **J.M. Lopez-Villegas:** Writing – review & editing, Visualization, Validation, Supervision, Methodology, Investigation, Conceptualization. **I. Cairó:** Validation, Resources, Methodology, Investigation, Data curation. **A. Garcia-Miquel:** Investigation, Conceptualization. **J. Romeu:** Writing – review & editing, Conceptualization. **L.L. Jofre:** Writing – review & editing, Conceptualization.

Declaration of competing interest

The authors declare the following financial interests/personal relationships which may be considered as potential competing interests: [Neus Vidal reports a relationship with University of Barcelona that includes: employment. No If there are other authors, they declare that they have no known competing financial interests or personal relationships that could have appeared to influence the work reported in this paper].

Acknowledgment

This work was supported by grants PID2021-124638OB-I00 funded by MCIN/AEI/10.13039/501100011033 and, F2I-PdCl-2022-004 founded by Fundació Bosch i Gimpera/UB.

Data availability

Data will be made available on request.

References

[1] U.S. Geological Survey, Mineral commodity summaries 2024, U.S. Geological Survey, 2024, pp. 212. doi: 10.3133/mcs2024.
[2] S. Popovics, Concrete materials - properties, Spec. Test. (1992).
[3] S. Taheri, A review on five key sensors for monitoring of concrete structures, Constr. Build. Mater. 204 (2019) 492–509, https://doi.org/10.1016/j.conbuildmat.2019.01.172.
[4] A. Wahab, M.M.A. Aziz, A.R.M. Sam, K.Y. You, A.Q. Bhatti, K.A. Kassim, Review on microwave nondestructive testing techniques and its applications in concrete technology, Constr. Build. Mater. 209 (2019) 135–146, https://doi.org/10.1016/j.conbuildmat.2019.03.110.
[5] P. Juan-García, J.M. Torrents, Measurement of mortar permittivity during setting using a coplanar waveguide, Meas. Sci. Technol. 21 (4) (2010) 045702, https://doi.org/10.1088/0957-0233/21/4/045702.
[6] K. Chung, S. Kharkovsky, Measurements of microwave reflection properties of early-age concrete and mortar specimens, IEEE Instrum. Meas. Technol. Conf. (2014) 1295–1300, https://doi.org/10.1109/I2MTC.2014.6860954.
[7] A. Wahab, M.M.A. Aziz, A.R.M. Mohd Sam, K.Y. You, Application of microwave waveguide techniques for investigating the effect of concrete dielectric and reflection properties during curing, J. Build. Eng. 38 (2021) 102209, https://doi.org/10.1016/j.jobe.2021.102209.
[8] L. Franceschelli, et al., Non-intrusive microwave technique for direct detection of concrete compressive strength monitoring by multivariate modeling, Measurement 206 (2023) 112332, https://doi.org/10.1016/j.measurement.2022.112332.
[9] A. Ahmadihaji, R. Izquierdo, A. Shih, From chip-based to chipless RFID sensors: a review, IEEE Sens. J. 23 (11) (2023) 11356–11373, https://doi.org/10.1109/JSEN.2023.3266316.
[10] C. Walther, F. Alkam, L. Nguyen-Tuan, M. Lieboldt, T. Lahmer, Challenges for embedding RFID sensors in reinforced concrete for low-effort structural health monitoring, ce/papers 6 (6) (2023) 1460–1469, https://doi.org/10.1002/cepa.2893.
[11] S. Johann, C. Strangfeld, M. Müller, B. Mieller, M. Bartholmai, RFID sensor systems embedded in concrete – requirements for long-term operation, Mater. Today Proc. 4 (5) (2017) 5827–5832, https://doi.org/10.1016/j.matpr.2017.06.053. Part 1.
[12] C. Strangfeld, S. Johann, M. Bartholmai, Smart RFID sensors embedded in building structures for early damage detection and long-term monitoring, Sensors 19 (24) (2019) 5514, https://doi.org/10.3390/s19245514.
[13] S. Johann, F. Baensch, P. Sturm, C. Tiebe, S. Pötschke, V. Lay, HF RFID-based measurement comparison for method optimization in M2 concrete and alkali-activated mortars, Mater. Today Proc. 62 (2022) 2571–2576, https://doi.org/10.1016/j.matpr.2022.03.465.

[14] S. Suresh, G. Chakaravarthi, A novel passive wireless RFID sensor for localized surface crack characterization on metals, Measurement 231 (2024) 114651, https://doi.org/10.1016/j.measurement.2024.114651.
[15] Y. Liu, F. Deng, Y. He, B. Li, Z. Liang, S. Zhou, Novel concrete temperature monitoring method based on an embedded passive RFID sensor tag, Sensors 17 (7) (2017) 1463, https://doi.org/10.3390/s17071463.
[16] G. González-López, J. Romeu, I. Cairó, I. Segura, T. Ikumi, L. Jofre-Roca, Wireless sensing of concrete setting process, Sensors 20 (20) (2020) 5965, https://doi.org/10.3390/s20205965.
[17] T. Ikumi, I. Cairó, J. Groeneveld, A. Aguado, A. de la Fuente, Embedded wireless sensor for in situ concrete internal relative humidity monitoring, Sensors 24 (6) (2024) 1756, https://doi.org/10.3390/s24061756.
[18] L. Presa Madrigal, J.A. Rodríguez Rama, D. AMartín Sánchez, J.L. Costafreda Mustelier, M.A. Sanjuán, J.L. Parra y Alfaro, Cost-effective temperature sensor for monitoring the setting time of concrete, Appl. Sci. 14 (2024) 4344, https://doi.org/10.3390/app14114344.
[19] M. Komary, P. Bajić, N. Tošić, A. De la Fuente, J. Turmo, Development of a low-cost IoT-based sensor for early-stage concrete monitoring, Procedia Struct. Integr. 64 (2024) 1311–1317, https://doi.org/10.1016/j.prostr.2024.09.202.
[20] M. Civera, A. Naseem, B. Chiaia, Recent advances in embedded technologies and self-sensing concrete for structural health monitoring, Struct. Concr. (2024), https://doi.org/10.1002/suco.202400714.
[21] S.-C. Ran, Q.-A. Wang, J.-F. Wang, Y.-Q. Ni, Z.-X. Guo, Y. Luo, A concise state-of-the-art review of crack monitoring enabled by RFID technology, Appl. Sci. 14 (2024) 3213, https://doi.org/10.3390/app14083213.
[22] N. Makul, Dielectric permittivity of various cement-based materials during the first 24 hours hydration, Open J. Inorg. Non-Metallic Mater. 3 (2013) 53–57, https://doi.org/10.4236/ojinm.2013.34009.
[23] N. Piladaeng, N. Angkawisittpan, S. Homwuttiwong, Determination of relationship between dielectric properties, compressive strength, and age of concrete with rice husk ash using planar coaxial probe, Meas. Sci. Rev. 16 (2016) 14–20, https://doi.org/10.1515/msr-2016-0003.
[24] A.K. Skrivervik, F. Merli, Design strategies for implantable antennas, in Loughborough Antennas and Propagation Conference, 2011, pp. 1–5. doi: 10.1109/LAPC.2011.6114011.
[25] J. Romeu, G. González-López, S. Blanch, L. Jofre, Antenna packaging for in-body applications, in 14th European Conference on Antennas and Propagation (EuCAP), 2020, pp. 1–5. doi: 10.23919/EuCAP48036.2020.9135889.
[26] X. Li, S. Xue, L. Xie, L. Pang, G. Wan, R. Li, A patch-antenna-based smart aggregate for passive strain sensing in concrete, J. Build. Eng. 94 (2024) 109931, https://doi.org/10.1016/j.jobe.2024.109931.
[27] D. Helena, A. Ramos, T. Varum, J.N. Matos, Antenna design using modern additive manufacturing technology: a review, IEEE Access 8 (2020) 177064–177083, https://doi.org/10.1109/ACCESS.2020.3027383.
[28] N. Vidal, J.M. Lopez-Villegas, J. Romeu, A. Salas Barenys, L. Jofre, 3D-printed UHF-RFID tag for embedded applications, IEEE Access 8 (2020) 146640–146647, https://doi.org/10.1109/ACCESS.2020.3015335.
[29] A.K. Skrivervik, Implantable antennas: The challenge of efficiency, In: 7th European Conference on Antennas and Propagation (EuCAP), 2013, pp. 3627–3631.
[30] ChatuTech, https://www.chatu-tech.com/en/home/.
[31] WitekLab, Online monitoring of the process of concrete setting in real time. Recuperado de https://www.witeklab.com/en/online-monitoring-of-the-process-of-concrete-setting-in-real-time/.
[32] G. González-López, S. Blanch, J. Romeu, L. Jofre, Debye frequency-extended waveguide permittivity extraction for high complex permittivity materials: concrete setting process characterization, IEEE Trans. Instrum. Meas. 69 (8) (2020) 5604–5613, https://doi.org/10.1109/TIM.2019.2957895.
[33] J.M. Lopez-Villegas, N. Vidal, J. Sieiro, A. Salas, B. Medina, F.M. Ramos, Study of 3-D printed conical inductors for broadband RF applications, IEEE Trans. Microw. Theory Tech. 66 (8) (2018) 3597–3602, https://doi.org/10.1109/TMTT.2018.2845862.
[34] V. Makarovaite, A.J.R. Hillier, S.J. Holder, C.W. Gourlay, J.C. Batchelor, Passive wireless UHF RFID antenna label for sensing dielectric properties of aqueous and organic liquids, IEEE Sens. J. 19 (11) (2019) 4299–4307, https://doi.org/10.1109/JSEN.2019.2896481.
[35] EM Microelectronic, 18000-63 Type C (Gen2) and 18000-63 Type C/18000-64 Type D (Gen2/TOTAL) RFIDIC. Recuperado de https://www.emmicroelectronic.com/product/epc-and-uhf-ics/em4325.
[36] NORDIC ID, NUR-10W RFID MODULES, https://www.nordicid.com/device/modules/.
[37] UNE-EN 196-1:2005, Métodos de ensayo de cementos. Parte 1: Determinación de resistencias mecánicas, AENOR, Madrid, Spain (2005).